

RESEARCH ARTICLE

MicroRNA-96-5p promotes proliferation, invasion and EMT of oral carcinoma cells by directly targeting FOXF2

Haiyan Wang¹, Ning Ma², Wenyue Li¹ and Zuomin Wang^{1,*}

ABSTRACT

Recently, microRNA-96-5p (miR-96-5p) has been reported to function as both a tumor suppressor and oncogene in several cancer types, including gastric cancer, hepatocellular cancer and lung cancer. However, the biological function of miR-96-5p and its precise mechanisms in oral squamous cell carcinoma (OSCC) have not been well clarified. The aim of this study was to study the roles of miR-96-5p/FOXF2 axis in OSCC. In this study, the miR-96-5p level was dramatically enhanced in OSCC tissues and cell lines, and the FOXF2 expression was significantly reduced. In addition, the FOXF2 expression was negatively related to the miR-96-5p level in OSCC tissues. Furthermore, downregulation of miR-96-5p obviously restrained OSCC cell proliferation, invasion and EMT. We confirmed that miR-96-5p could directly target FOXF2 by luciferase reporter assay. Moreover, knockdown of FOXF2 also could markedly promote the proliferation, invasion and EMT of OSCC cells. Finally, overexpression of FOXF2 in OSCC cells partially reversed the promoted effects of miR-96-5p mimic. Knockdown of miR-96-5p restrained OSCC cells proliferation, invasion and EMT via regulation of FOXF2.

KEY WORDS: Oral squamous cell carcinoma, MicroRNA-96-5p, FOXF2, Proliferation, Invasion

INTRODUCTION

Head and neck squamous cell carcinoma (HNSCC) is the sixth most common cancer worldwide. It is reported that 1.6 million new cases of HNSCC are diagnosed each year, and half of HNSCC is oral squamous cell carcinoma (OSCC) with 333,000 deaths (Warnakulasuriya, 2009). Although there are several therapeutic treatments such as chemotherapy combined with radical surgery and surgery combined with radiation, the 5-year survival rate of OSCC is only approximately 50% (Leemans et al., 2011). The pathogenesis of OSCC is complex, and many genes and pathways are involved in it. However, the mechanism of OSCC development remains unclear.

MicroRNAs (miRNAs) are a family of small, endogenous noncoding RNAs. They regulate the translation or induce degradation of specific protein coding genes through binding to the 3'-untranslated regions of the mRNA (Ambros, 2004). According to bioinformatic analysis, it was predicted that miRNAs targeted more

than 60% of human genes (Xu et al., 2014). Previous reports demonstrated that altered miRNA expression participated in tumorigenesis and the development of various cancers (He et al., 2005, 2007; Feng et al., 2018). Thus, miRNAs are thought to be markers of cancer diagnosis, progression and prognosis (Bartels and Tsongalis, 2009). Many human miRNAs have been confirmed to be dysregulated in OSCC, including miR-543, miR-4513, miR-31, miR-223 and miR-125b (Wang et al., 2019; Xu et al., 2019; Kao et al., 2019; Jiang et al., 2019; Chen et al., 2019). Up until now, miR-96-5p had been reported to function as an oncogene in ovarian cancer, HNSCC, hepatocellular carcinoma (Liu et al., 2019; Vahabi et al., 2019; Iwai et al., 2018), or function as a tumor suppressor in colorectal cancer (Ress et al., 2015), the functions of miR-96-5p in OSCC were rarely explored previously. Therefore, we investigated the functional roles and mechanisms of miR-96-5p in OSCC.

Forkhead transcription factors are characterized by a winged helix DNA-binding domain and are essential for embryogenesis (Kaufmann and Knöchel, 1996). Some of them, such as FOXQ1, FOXQ3 and FOXO1, have been identified as regulating tumorigenesis and tumor progression (Mottok et al., 2018; Saito et al., 2016; Chae et al., 2019). It has been reported that the Forkhead box F2 transcription factor (FOXF2) functions as tumor suppressor in breast cancer, gastric cancer, colorectal cancer, lung cancer and hepatocellular carcinoma (Cai et al., 2015; Higashimori et al., 2018; Zhang et al., 2015; Kundu et al., 2016; Shi et al., 2016). However, the expression of FOXF2 and its functional roles in OSCC are still unknown.

Here, in order to investigate the functional role of miR-96-5p in OSCC, we detected the miR-96-5p level in OSCC tissues and cell lines. Next, we predicted that miR-96-5p directly targeted FOXF2 according to the online database TargetScan 7.2. For further study, we explored the relationship between miR-96-5p and FOXF2 in OSCC tissues. Lastly, the effects of miR-96-5p or FOXF2 overexpression on proliferation, invasion and EMT of OSCC cells were determined.

RESULTS

High level of miR-96-5p in OSCC tissues and cells


In this study, the miR-96-5p level in OSCC tissues and cells were detected by using qRT-PCR. Our findings demonstrated that the miR-96-5p level in the OSCC tissues was higher than that in the adjacent tissues (Fig. 1A). Next, the data further confirmed that the miR-96-5p level was higher in Tca8113 and Cal-27 cells than that in the other three OSCC cell lines (Fig. 1B). Therefore, Tca8113 and Cal-27 cells were used in the following experiments.

The effect of miR-96-5p on proliferation of OSCC cells

After transfection with miR-96-5p mimic or inhibitor, the results showed that the miR-96-5p level was significantly upregulated or downregulated in a miR-96-5p mimic or inhibitor group compared to a negative control (NC) group (Fig. 2A), respectively. To study

¹Department of Stomatology, Beijing Chaoyang Hospital, Capital Medical University, Beijing 100020, China. ²Department of Stomatology, Qingdao Municipal Hospital, Qingdao 266011, China.

*Author for correspondence (wangzuominchaoyang@163.com)

 H.W., 0000-0003-2100-3924; N.M., 0000-0001-8570-4266; Z.W., 0000-0001-8803-8406

This is an Open Access article distributed under the terms of the Creative Commons Attribution License (<https://creativecommons.org/licenses/by/4.0>), which permits unrestricted use, distribution and reproduction in any medium provided that the original work is properly attributed.

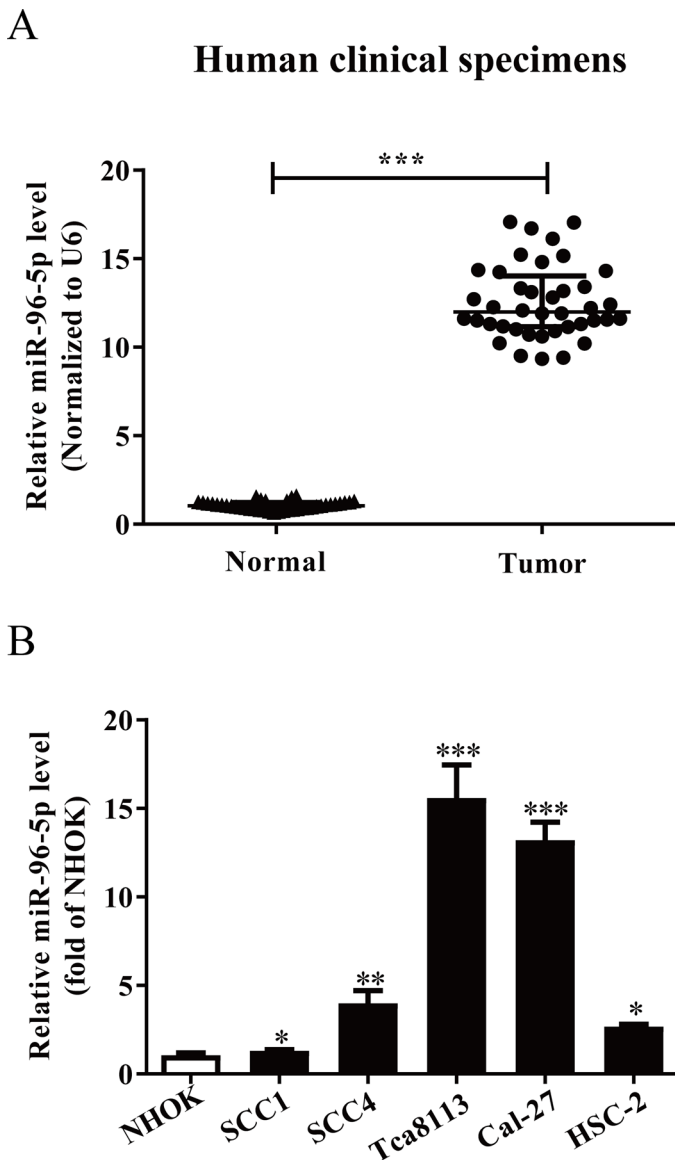


Fig. 1. The levels of miR-96-5p in OSCC tissues and cell lines. (A) Quantitative RT-PCR analysis of miR-96-5p level in OSCC tissues and adjacent normal tissues ($n=40$). Transcript levels were normalized to U6 level. (B) Relative miR-96-5p level analyzed via quantitative RT-PCR in five OSCC cell lines normalized to U6 ($n=6$). All data are presented as means \pm s.e.m. * $P<0.05$, ** $P<0.01$, *** $P<0.001$ versus normal tissues or NHOK.

the role of miR-96-5p in regulating Tca8113 and Cal-27 cell proliferation, our results suggested that the introduction of miR-96-5p significantly promoted Tca8113 and Cal-27 cells proliferation (Fig. 2B). However, transfection with miR-96-5p inhibitor suppressed the cell proliferation of Tca8113 and Cal-27 cells compared with the NC group (Fig. 2B). Next, overexpression of miR-96-5p enhanced expression of CDK4 and cyclin D1 and reduced the expression of p27 at mRNA level (Fig. 2C). In addition, downregulation of miR-96-5p had the opposite effect on regulating expression of these cell cycle genes (Fig. 2C).

The effects of miR-96-5p on invasion and EMT in OSCC cells

Compared to the NC group, the results from the Transwell assays showed that increased miR-96-5p level significantly enhanced the number of invading OSCC cells (Fig. 3A). In addition, we detected

MMP-2, MMP-9 and TIMP-1 expression by ELISA and qRT-PCR assays. The results indicated that MMP-2 and MMP-9 expression were markedly increased by enhancing miR-96-5p level in Tca8113 and Cal-27 cells (Fig. 3B,C), while expression of TIMP-1 was dramatically decreased (Fig. 3B,C). Finally, our results suggested that the epithelial marker E-cadherin was significantly decreased after overexpression of miR-96-5p. By contrast, introduction of miR-802 increased the mesenchymal markers N-cadherin and Vimentin expression (Fig. 4), while the miR-96-5p inhibitors showed the opposite effect (Fig. 4). Taken together, we demonstrated that miR-96-5p could promote the progression of OSCC by repressing proliferation, invasion and EMT of OSCC cells.

miR-96-5p directly targeted FOXF2 3'UTR

We found a miR-96-5p binding site in the 3'UTR of FOXF2 by using TargetScan 7.2 online database (Fig. 5A). Then, we found that FOXF2, a critical oncogene, is a direct target of miR-96-5p by luciferase reporter assay. Introduction of miR-96-5p significantly suppressed WT FOXF2 reporter activity but not the activity of the mutated reporter construct in Tca8113 and Cal-27 cells, suggesting that miR-96-5p could specifically target the FOXF2 3'UTR by binding to the seed sequence (Fig. 5B). Upregulation of miR-96-5p could significantly reduce FOXF2 expression, whereas downregulation of miR-96-5p enhanced FOXF2 expression (Fig. 5C). These results suggested that miR-96-5p directly targeted FOXF2 through 3'UTR sequence binding.

Next, FOXF2 expression was detected by qRT-PCR in OSCC tissues. Our results demonstrated that FOXF2 expression was obviously downregulated in OSCC tissues compared with the adjacent tissues (Fig. 5D). Next, we also determined the FOXF2 expression in five OSCC cell lines (such as SCC1, SCC4, Tca8113, Cal-27 and HSC-2) and a human normal oral keratinocyte cell culture (NHOK). The FOXF2 expression in Tca8113 and Cal-27 cells was lower than that in the other three cell lines (Fig. 5E). Finally, Pearson's correlation analysis revealed a significant inverse correlation between FOXF2 and miR-96-5p in OSCC tissues (Fig. 5F). From the above data, we predicted that miR-96-5p might negatively regulate FOXF2 expression.

Knockdown of FOXF2 promoted OSCC cells proliferation, invasion and EMT

To investigate the functional roles of FOXF2 in OSCC cells, the proliferation and invasion of OSCC cells were detected after transfection with si-NC or si-FOXF2. Transfection with si-FOXF2 significantly decreased the FOXF2 expression in Tca8113 and Cal-27 cells compared with the si-NC group (Fig. 6A). Then, we found that silencing FOXF2 evidently promoted the proliferation of Tca8113 and Cal-27 cells (Fig. 6B). Next, a Transwell assay revealed that decreased FOXF2 expression accelerated invasion of Tca8113 and Cal-27 cells (Fig. 6C). Moreover, knockdown of FOXF2 markedly upregulated expression of MMP-2 and MMP-9, and downregulated expression of TIMP-1 in Tca8113 and Cal-27 cells (Fig. 6D). For further study, downregulation of FOXF2 reduced the expression of E-cadherin, and enhanced the expression of N-cadherin and Vimentin (Fig. 6E). Consequently, silencing FOXF2 remarkably restrained OSCC cell proliferation, invasion and EMT.

miR-96-5p markedly promoted the proliferation, invasion and EMT of OSCC cells through regulating FOXF2 expression

To determine whether miR-96-5p regulated the proliferation, invasion and EMT of OSCC cells by directly targeting FOXF2,

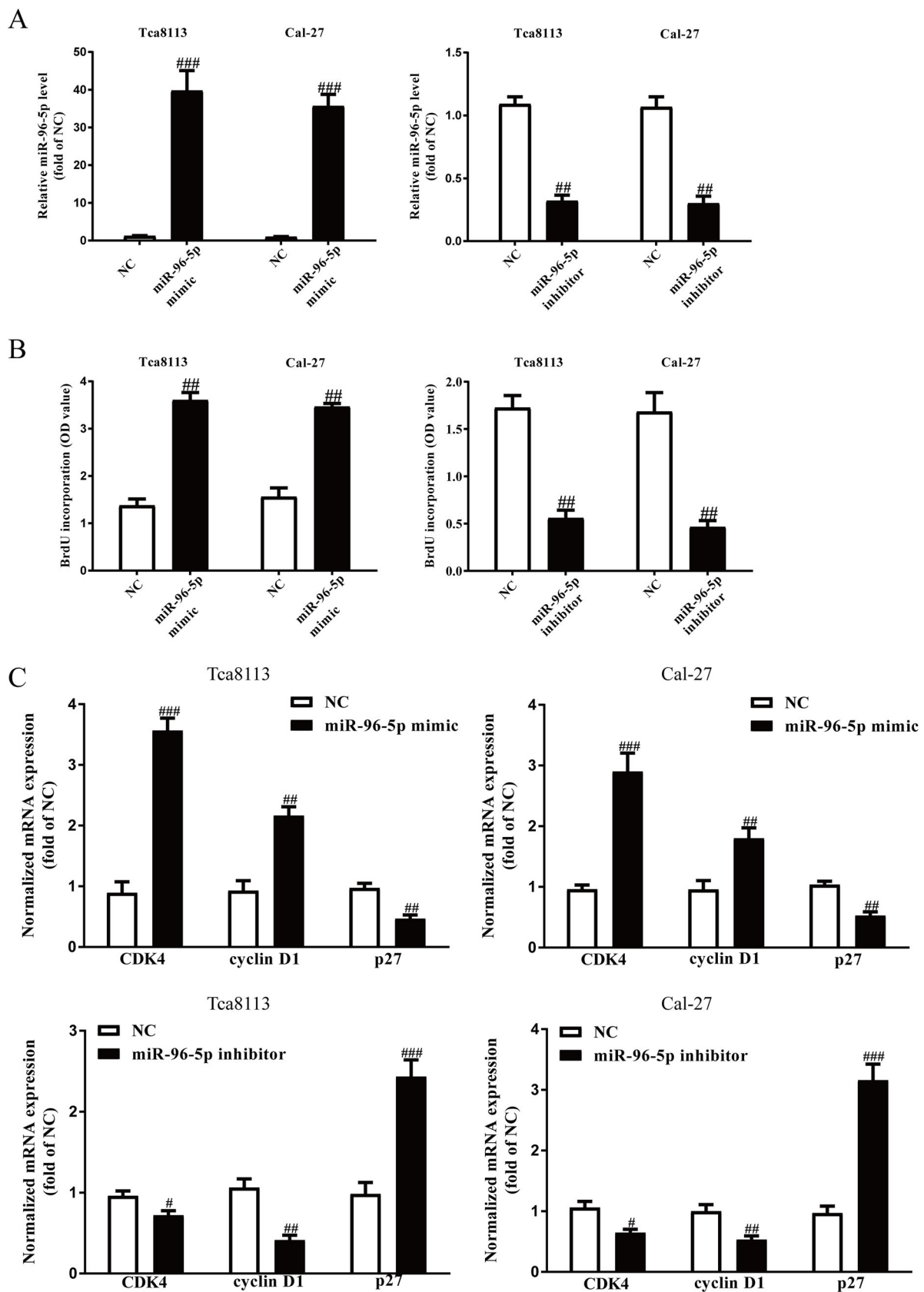


Fig. 2. The effects of miR-96-5p on proliferation and related molecules in OSCC cells. Tca8113 and Cal-27 cells were transfected with miR-96-5p mimic or inhibitor for 48 h. (A) The level of miR-96-5p was detected by quantitative RT-PCR. (B) Cell proliferation was assessed by a BrdU-ELISA assay. (C) The mRNA expression of CDK4, cyclin D1 and p27 were determined by quantitative RT-PCR. All data are presented as means±s.e.m., $n=6$. # $P<0.05$, ## $P<0.01$, ### $P<0.001$ versus NC.

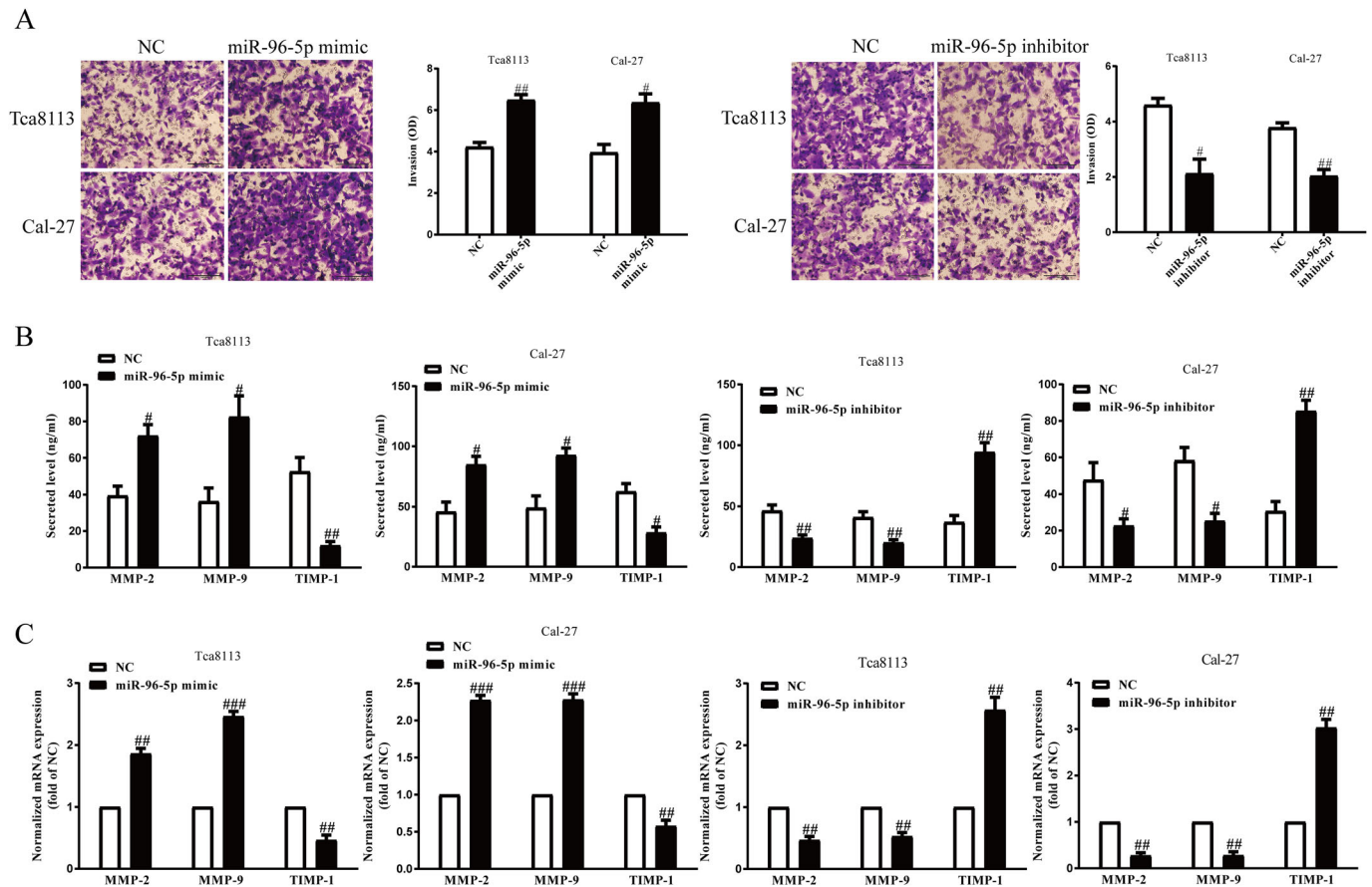


Fig. 3. The effects of miR-96-5p on the invasion and related molecules expression in OSCC cells. Tca8113 and Cal-27 cells were transfected with miR-96-5p mimic or inhibitor for 48 h. (A) The invasion was assessed by Transwell assay. (B) Total secretions of MMP-2, MMP-9 and TIMP-1 in the culture supernatants were detected by ELISA assays. (C) The mRNA expression of MMP-2, MMP-9 and TIMP-1 were examined by qRT-PCR. All data are presented as means \pm s.e.m., $n=6$. [#] $P<0.05$, ^{##} $P<0.01$ versus NC.

we co-transfected NC or miR-96-5p mimic with pcDNA3.1 or pcDNA-FOXF2 into Tca8113 and Cal-27 cells (Fig. 7A). Overexpression of FOXF2 abrogated the promoted effect of miR-96-5p mimic on cell proliferation (Fig. 7B). At the same time, expression of cyclin D1 and CDK4 was decreased and expression of p27 was increased in miR-96-5p-overexpressing Tca8113 and Cal-27 cells after exogenous FOXF2 upregulation (Fig. 7C). Next, the data showed that FOXF2 overexpression partially reversed the invasion of Tca8113 and Cal-27 cells promoted by miR-96-5p mimic (Fig. 7D) through decreasing MMP-2 and MMP-9 expression and increasing TIMP-1 expression (Fig. 7E). Next, overexpression of FOXF2 inhibited miR-96-5p mimic-induced EMT of OSCC cells (Fig. 7F). Hence, the promoted effects of miR-96-5p mimic were reversed by overexpression of FOXF2. Altogether, all the above results suggested that overexpression of miR-96-5p promoted OSCC cell proliferation, invasion and EMT via directly downregulating FOXF2 expression.

DISCUSSION

miRNAs serve as important regulatory factors, which affect OSCC progression. Jiang et al. reported that MiR-223 promotes OSCC proliferation and migration by regulating FBXW7 (Jiang et al., 2019). Chen et al. indicated that miR-125b suppresses oral oncogenicity by targeting the anti-oxidative gene PRXL2A (Chen et al., 2019). Numerous studies have found that miR-96-5p not only affected cell

proliferation, but was also closely associated with prognosis in cancers including ovarian cancer, HNSCC, hepatocellular carcinoma and colorectal cancer (Liu et al., 2019; Vahabi et al., 2019; Iwai et al., 2018; Ress et al., 2015).

In this study, our results showed that the miR-96-5p level was upregulated in OSCC tissues compared with the adjacent normal tissues. In addition, miR-96-5p level was also upregulated in OSCC cell lines compared with NHOK cells. Moreover, we, for the first time, explored the functional roles of miR-96-5p in OSCC cells. We found that overexpression of miR-96-5p more significantly promoted OSCC cell proliferation than the cells transfected with NC, whereas downregulation of miR-96-5p inhibited OSCC cell proliferation. Cell cycle regulation involved complex events, such events revealed that cell cycle related proteins provided a promising mechanism for the inhibition of growth (Qiu et al., 2017; Wang et al., 2015). An earlier study suggested that the upregulation of cyclin-dependent kinases (CDKs) and cyclin (D1 and E1) participated in cell cycle progression and arrested cells at the G0/G1 phase (Wang et al., 2015). p21 and p27 have been reported as inhibitors of CDK protein with an anti-proliferative effect on mesangial cells (Wang et al., 2011). Here, we also found that introduction of miR-96-5p enhanced expression of CDK4 and cyclin D1, while it also reduced p27 expression.

Invasion is one process of metastasis. Here, the data indicated that an increased or decreased miR-96-5p level significantly inhibited or

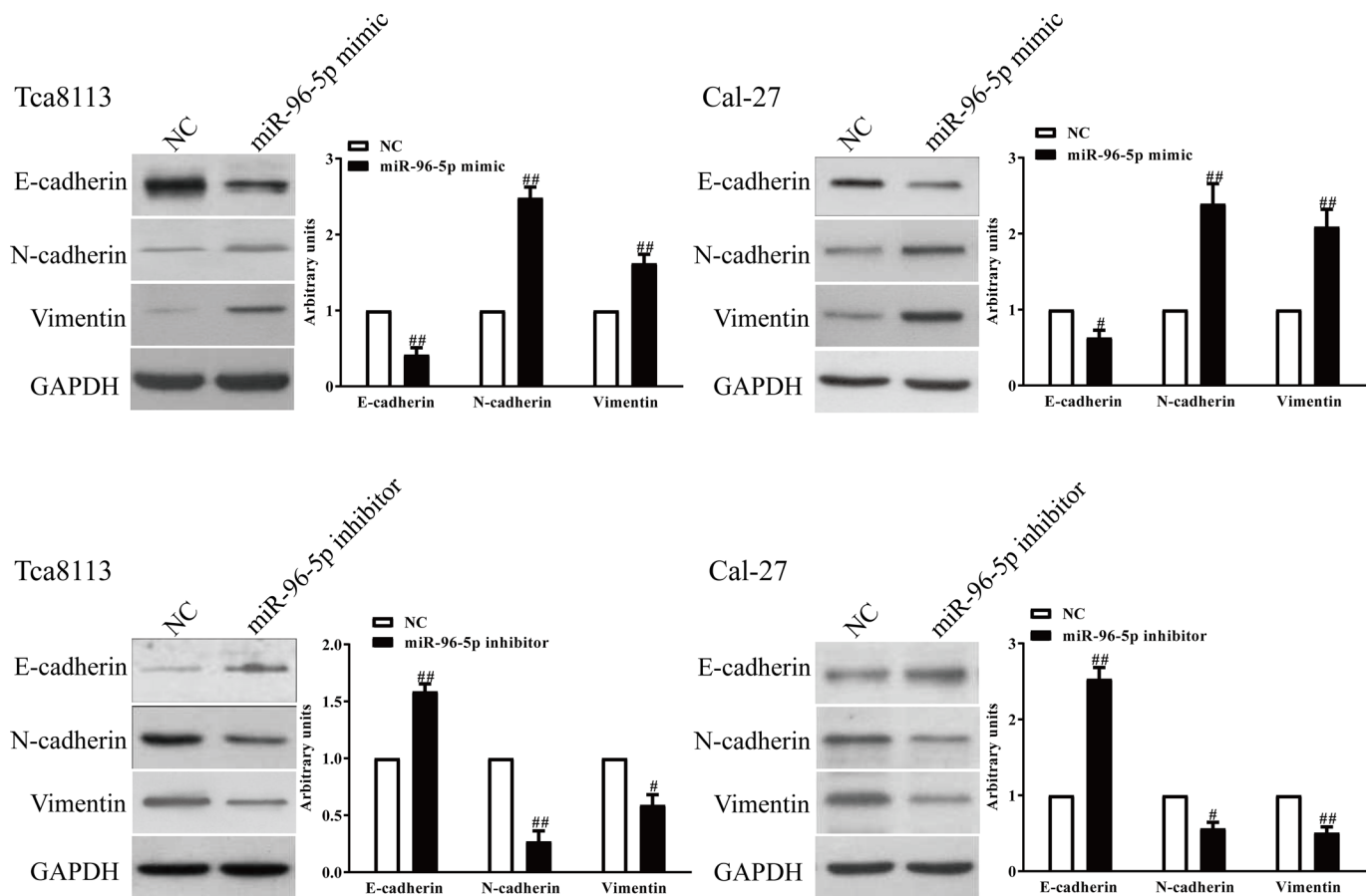


Fig. 4. Effects of miR-96-5p on the EMT of OSCC cells. Tca8113 and Cal-27 cells were transfected with miR-96-5p mimic or inhibitor for 48 h. The expression of E-cadherin, Vimentin and N-cadherin were detected by western blot assays. All data are presented as mean \pm s.e.m., $n=6$. # $P<0.05$, ## $P<0.01$ versus NC.

enhanced, respectively, the invasive ability of SCC1 cells compared with the control group. Furthermore, one very important step in cancer cell invasion is that proteolytic enzymes degrade the extracellular matrix (ECM) components (Simpson-Haidaris and Rybarczyk, 2001). Moreover, the MMPs degrading the ECM process contributes to cancer cell angiogenesis, invasion and metastasis (Bogenrieder and Herlyn, 2003; Vihinen and Kähäri, 2002; Sounni et al., 2003). Both MMP-2 and MMP-9 degrade components of the basement membrane to promote cancer invasion (Vihinen and Kähäri, 2002; Hornebeck et al., 2002; Klein et al., 2004). Moreover, it is reported that the imbalance between TIMPs and MMPs is important in the early stages of tumor progression (Herszényi et al., 2012). Next, upregulation of miR-96-5p significantly decreased expression of MMP-2 and MMP-9, and increased TIMP-1 expression in Tca8113 and Cal-27 cells, whereas downregulation of miR-96-5p enhanced both MMP-2 and MMP-9 expression and reduced TIMP-1 expression. The EMT process has been confirmed to be critical in cell invasion in types of cancer (Christiansen and Rajasekaran, 2006). At the molecular level, EMT is characterized by downregulation of the epithelial marker E-cadherin and cytokeratins, with upregulation of mesenchymal markers like N-cadherin, Vimentin and fibronectin (Yao et al., 2011; Gheldof and Berx, 2013). We found that the introduction of miR-96-5p promoted the EMT of OSCC cells by decreasing E-cadherin expression and increasing N-cadherin and Vimentin expression. All the above results indicated

that miR-96-5p restrained cell proliferation, invasion and EMT of OSCC.

It is well known that miRNAs perform their function by regulating the expression of their target gene. Thus, we explore the functional target gene for miR-96-5p, which is involved in OSCC progression. TargetScan and luciferase reporter assay suggested that FOXF2 might be the functional target gene of miR-96-5p. Furthermore, increased expression or knockdown of miR-96-5p significantly inhibited or promoted FOXF2 expression, respectively. FOXF2 is a tumor suppressor and participates in the development and progression of multiple cancers (Cai et al., 2015; Higashimori et al., 2018; Zhang et al., 2015; Kundu et al., 2016; Shi et al., 2016). In our study, we also observed that FOXF2 expression was frequently at low levels in tumor tissue when compared with its paired non-tumor tissue, which agreed with previous studies in breast cancer, gastric cancer, colorectal cancer, lung cancer and hepatocellular carcinoma (Cai et al., 2015; Higashimori et al., 2018; Zhang et al., 2015; Kundu et al., 2016; Shi et al., 2016). Hence, our results indicated that FOXF2 expression might play a cardinal role in tumorigenesis of OSCC. Besides, miR-96-5p level was inversely correlated with FOXF2 expression in OSCC. Moreover, the data showed that silencing FOXF2 could restrain the proliferation, invasion and EMT of OSCC cells. Next, our results showed that overexpression of FOXF2 inhibited the proliferation, invasion and EMT of OSCC cells promoted by upregulation of miR-96-5p. Our findings

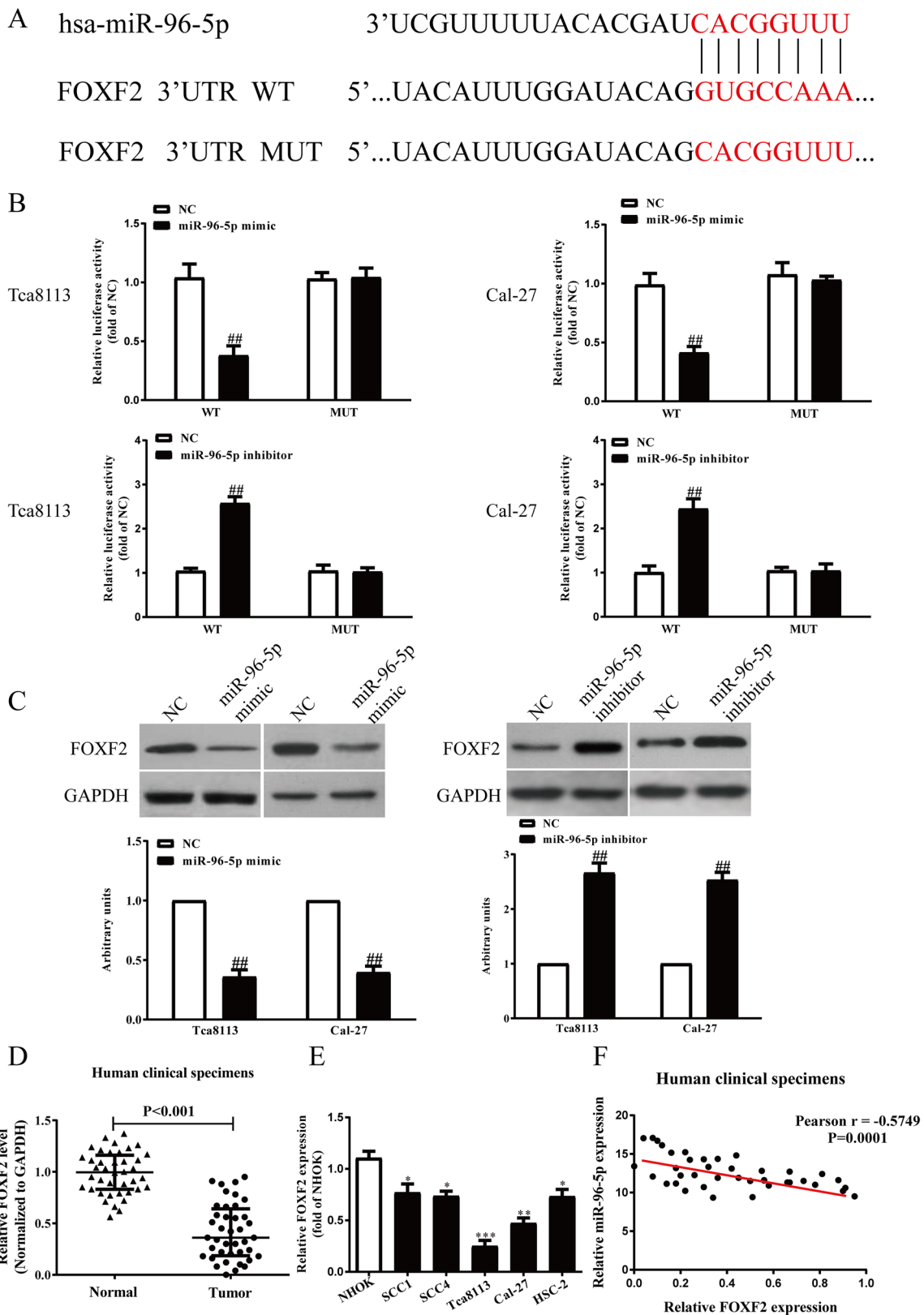


Fig. 5. FOXF2 is a direct target of miR-96-5p. Tca8113 and Cal-27 cells were transfected with miR-96-5p mimic or inhibitor for 48 h. (A) Schematic representation of FOXF2 3'UTRs showing putative miRNA target site. (B) The analysis of the relative luciferase activities of FOXF2-WT and FOXF2-MUT. (C) The protein expression of FOXF2 were determined by western blot assay. (D) Quantitative RT-PCR analysis of FOXF2 expression in OSCC tissues ($n=40$) and adjacent normal tissues ($n=40$). Transcript levels were normalized to GAPDH expression. (E) Relative FOXF2 expression analyzed via quantitative RT-PCR in five OSCC cell lines normalized to GAPDH ($n=6$). (F) Pearson's correlation analysis of the relative expression levels of miR-96-5p and the relative FOXF2 mRNA levels in OSCC tissues. All data are presented as means \pm s.e.m., $n=6$. ## $P<0.01$ versus NC; * $P<0.05$, ** $P<0.01$, *** $P<0.001$ versus normal tissues or NHOK.

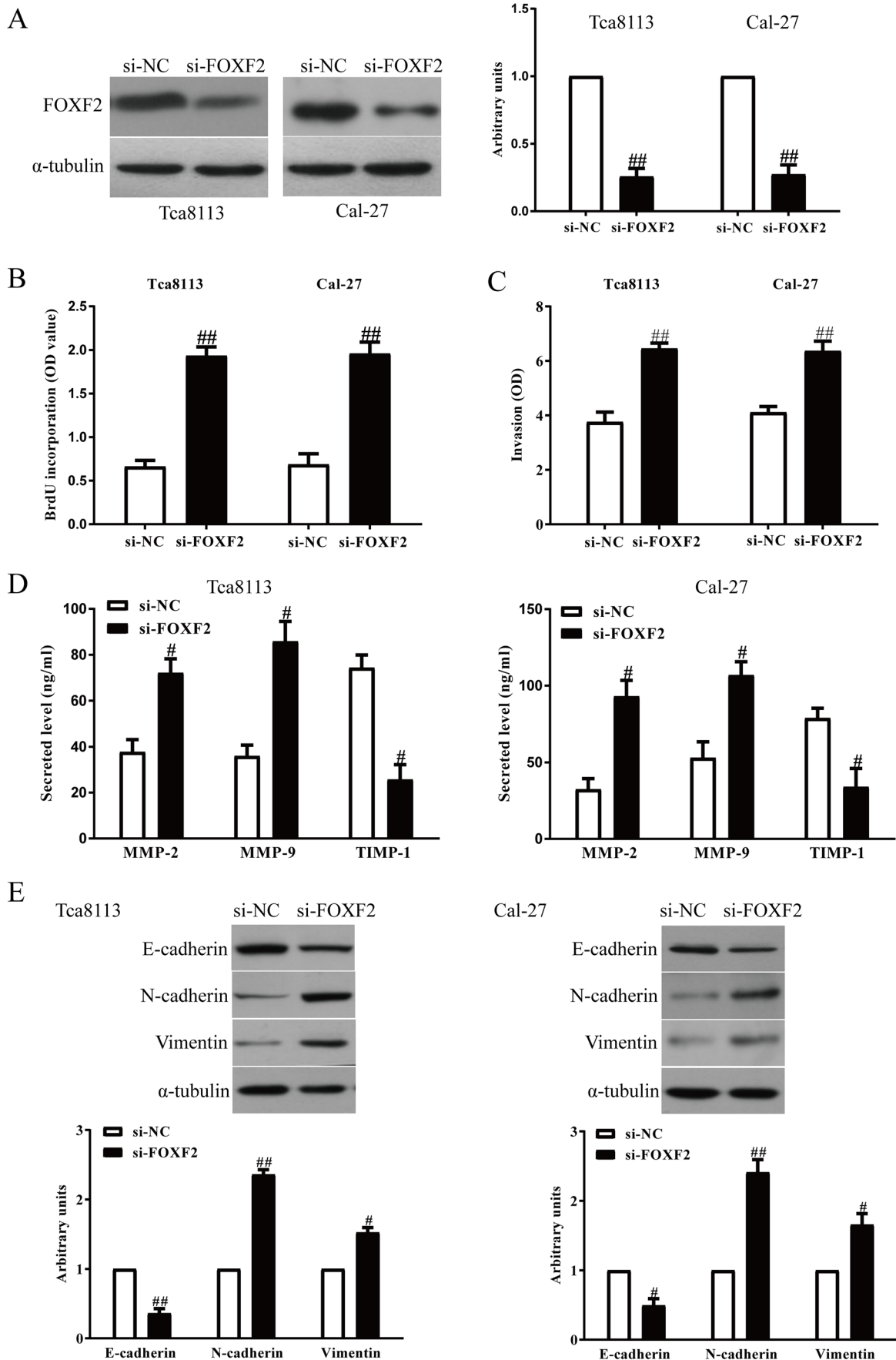


Fig. 6. See next page for legend.

Fig. 6. The effects of FOXF2 knockdown on the proliferation, invasion and EMT in OSCC cells. Tca8113 and Cal-27 cells were transfected with si-NC or si-FOXF2 for 48 h. (A) The protein expression of FOXF2 was determined by western blot. (B) Cell proliferation was assessed by a BrdU-ELISA assay. (C) The invasion of OSCC cells was assessed by Transwell assay. (D) Total secretions of MMP-2, MMP-9 and TIMP-1 in the culture supernatants were detected by ELISA assays. (E) The expression of E-cadherin, Vimentin and N-cadherin were detected by western blot assays. All data are presented as means±s.e.m., $n=6$. # $P<0.05$, ## $P<0.01$ versus si-NC.

demonstrated that miR-96-5p might act as an oncogene in OSCC by directly targeting FOXF2.

Altogether, the miR-96-5p level was dramatically upregulated and the FOXF2 expression was significantly downregulated in OSCC tissues. Introduction of miR-96-5p promoted proliferation, invasion and EMT of OSCC cells by directly downregulating FOXF2 expression. Hence, these findings suggested important roles for miR-96-5p/FOXF2 axis in the OSCC pathogenesis and its potential application in cancer therapy.

MATERIALS AND METHODS

Human tissue samples

Thirty pairs of human OSCC tissues and their adjacent non-cancer tissues were collected from patients at the Beijing Chaoyang Hospital, Capital Medical University between Feb 2018 and Feb 2019. All samples were immediately frozen in liquid nitrogen for subsequent quantitative RT-PCR and western blot analysis. All participants signed a written informed consent form. This study was approved by the Ethical Committee of Beijing Chaoyang Hospital, Capital Medical University (BCH2018011208) and complied with the guidelines and principles of the Declaration of Helsinki.

Cell culture

The human OSCC cell lines such as SCC1, SCC4, Tca8113, Cal-27, HSC-2 and the normal human oral keratinocyte cell lines (NHOK) were purchased from the American Type Culture Collection (ATCC, USA). All the cells were cultured in the DMEM/F12 medium (GIBCO, USA) containing 10% FBS (GIBCO, USA) and penicillin/streptomycin (100 U/ml and 100 mg/ml, respectively) (GIBCO, USA) at 37°C in a humidified atmosphere of 5% CO₂.

Transient transfection

The miR-96-5p mimics, miRNA-NC, miR-96-5p inhibitors, si-NC and si-FOXF2 were purchased from Gene-Pharma (Shanghai, China). The FOXF2-overexpression plasmid was generated by inserting FOXF2 cDNA into a pcDNA3.1 vector, which was sequenced and confirmed by Gene-Pharma. The miR-96-5p mimics, NC, miR-96-5p inhibitors, si-NC, si-FOXF2, pcDNA3.1 vector and FOXF2-overexpression plasmid were transfected using Lipofectamine 3000 reagent (Invitrogen, USA) per the manufacturer's protocols. Cells were transfected for 48 h, and total RNA and protein were collected.

Isolation of RNA and quantitative polymerase chain reaction analysis

Total RNA from OSCC cells were extracted using TRIzol (Invitrogen, USA) following the manufacturer's protocols. MiRNA-specific RT primers (RiboBio, Guangzhou, China) for miR-96-5p and random primers (TaKaRa, Dalian, China) for mRNAs were synthesized. Quantitative polymerase chain reaction (qPCR) was used to measure reverse-transcribed cDNA with SYBR Green PCR Kit (QIAGEN, Shanghai, China) under the following conditions: pre-denaturation at 95°C for 5 min, denaturation at 95°C for 10 s, annealing and extension at 60°C for 30 s, the followed steps were running for 40 cycles. The relative miRNA and mRNA expression levels were normalized by U6 and GAPDH, respectively. The relative expression levels of miR-96-5p, FOXF2, CDK4, cyclin D1, p27, MMP-2, MMP-9 and TIMP-1 were normalized to those of internal control U6 or

GAPDH using the comparative delta CT ($2^{-\Delta\Delta Ct}$) method. Prime sequences are shown in Table 1.

Protein extraction and western blot analysis

Transfected cells were lysed with RIPA lysis buffer (Thermo Fisher Scientific, USA) containing protease inhibitors (Thermo Fisher Scientific, USA). The concentration of extracted protein was measured by using a BCA protein assay kit (Thermo Fisher Scientific, USA). Equal amounts of protein were separated with 10% SDS-PAGE and transferred to polyvinylidene difluoride (PVDF) membranes (Millipore, USA). The membranes were then blocked with 5% non-fat milk (BD Biosciences, San Jose, USA) in TBST for 1 h at room temperature, followed by incubation with primary antibodies of FOXF2 (ab23306), cyclin D1 (ab16663), CDK4 (ab108357), p27 (ab32034), MMP-2 (ab97779), MMP-9 (ab38898) and TIMP-1 (ab109125) (Abcam, USA) overnight at 4°C. Subsequently, the membranes were washed with TBST three times and probed with the corresponding horseradish peroxidase-conjugated secondary antibodies (Cell Signaling Technology, USA) for 2 h at room temperature. ECL reagent (Pierce) was used to detect the signals on the membranes.

Transwell invasion assay

After transfection, cells were resuspended in serum-free DMEM/F12 medium, and then were seeded into the upper chamber (Corning, New York, USA) coated with matrigel (BD Biosciences, San Jose, USA), and medium containing 10% FBS was added into the bottom chamber. After incubation for 24 h, cells remaining on the upper membrane were carefully removed, and those migrating to the basal side of the membrane were fixed with 4% paraformaldehyde and stained with Crystal Violet (Sigma-Aldrich, St Louis, USA) for 30 min. Finally, migrated cells in random three visual fields were photographed and counted under a microscope (Olympus, Tokyo, Japan). Finally, the washing solution was examined at 540 nm for the counting of the number of OSCC cells.

Measurement of MMP-2, MMP-9 and TIMP-1 levels by ELISA assay

According to the protocol, the supernatants of OSCC cells were collected after treatment, and the concentrations of MMP-2, MMP-9 and TIMP-1 were measured using a sandwich ELISA kit (USCN, USCN Life Science, Wuhan, China) according to the manufacturer's instructions. Briefly, the primary antibody was coated onto ELISA plates and incubated for 2 h at room temperature. Samples and standards were added to the wells and incubated for 1 h. Then the wells were washed and a biotinylated antibody was added for 1 h. The wells were washed again, and streptavidin conjugated to horseradish peroxidase was added for 10 min. After washing, tetramethylbenzidine was added for color development and the reaction was terminated with 1 mol/l H₂SO₄. Absorbance was measured at 490 nm. Values were expressed as ng/ml.

Luciferase reporter assay

The luciferase reporter vectors (pGL3-FOXF2-3'UTR WT and pGL3-FOXF2-3'UTR MUT) were synthesized by GenePharma. OSCC cells were seeded into 24-well plates and transfected with pGL3-FOXF2-3'UTR WT or pGL3-FOXF2-3'UTR MUT, along with miR-96-5p mimics or miR-NC using Lipofectamine 3000 per the manufacturer's instructions. After transfection for 48 h, luciferase reporter assays were performed with the Promega Dual-Luciferase Reporter Assay System. The relative firefly luciferase activities were measured by normalizing to renilla luciferase activities.

Statistical analysis

The data were expressed as the means±standard error of the mean (s.e.m.). The number of independent experiments was represented by 'n'. Correlations between miR-96-5p and FOXF2 levels were analyzed using Pearson's correlation coefficient. Two-tailed Student's *t*-test was used for other comparisons. The associations between miR-96-5p level and clinicopathological features were analyzed using χ^2 test. $P<0.05$ was considered statistically significant.

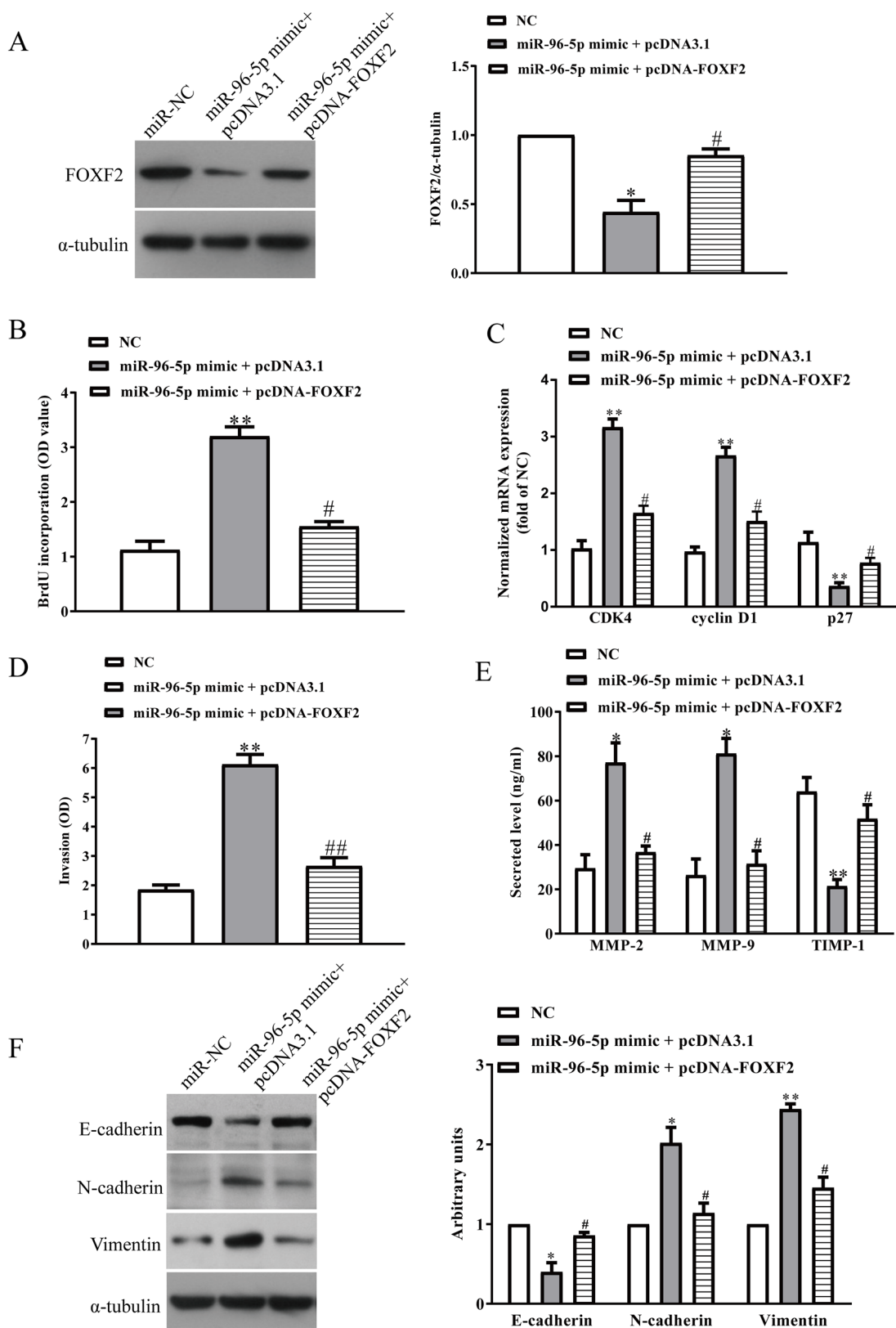


Fig. 7. Introduction of FOXF2 promoted cell proliferation and invasion in miR-96-5p-overexpressing OSCC cells. Tca8113 cells were co-transfected with pcDNA3.1 or pcDNA-FOXF2 with or without miR-96-5p mimic. (A) The protein expression of FOXF2 was determined by western blot assay. (B) Cell proliferation was assessed by a BrdU-ELISA assay. (C) The expression of CDK4, cyclin D1 and p27 were determined by quantitative RT-PCR, respectively. (D) The invasion of OSCC cells was assessed by Transwell assay. (E) Total secretions of MMP-2, MMP-9 and TIMP-1 in the culture supernatants were detected by ELISA assays. (F) The expression of E-cadherin, Vimentin and N-cadherin were detected by western blot assays. All data are presented as means \pm s.e.m., $n=6$. * $P<0.05$, ** $P<0.01$ versus NC; # $P<0.05$, ## $P<0.01$ versus miR-96-5p mimic+pcDNA3.1.

Table 1. Sequences of primers for qRT-PCR

Gene	Primer sequence
FOXF2	F: 5'-AATGCCACTCGCCCTACAC-3' R: 5'-CGTTCTGGTGAAGTAGCTCT-3'
CDK4	F: 5'-GGGGACCTAGAGCAACTTACT-3' R: 5'-CAGCGCAGTCTTCCAAT-3'
Cyclin D1	F: 5'-GCTGCGAAGTGGAAACATC-3' R: 5'-CCTCCTTCTGCACACATTTGAA-3'
p27	F: 5'-AACGTGCGAGTGTCTAACGG-3' R: 5'-CCCTCTAGGGGTTGTGATTCT-3'
MMP-2	F: 5'-TACAGGATCATTGGCTACACACC-3' R: 5'-GGTACATCGCTCCAGACT-3'
MMP-9	F: 5'-TGTACCGCTATGTTACTACTCG-3' R: 5'-GGCAGGGACAGTTGCTTCT-3'
TIMP-1	F: 5'-CTTCTGCAATTCGACCTCGT-3' R: 5'-ACGCTGGTATAAGGTGGTCTG-3'
miR-96-5p	F: 5'-TTTGGCACTAGCACATTTT-3' R: 5'-GAACATGTCTGCGTATCTC-3'
U6	F: 5'-CTCGTTCGGCAGCACA-3' R: 5'-AACGCTTACGAATTTGCGT-3'
GAPDH	F: 5'-GAGTCAACGGATTTGGCTGATTG-3' R: 5'-CCTGGAAGATGGTATGGGATT-3'

Competing interests

The authors declare no competing or financial interests.

Author contributions

Conceptualization: Z.W.; Methodology: H.W., N.M., W.L.; Software: H.W., N.M., W.L.; Validation: H.W.; Formal analysis: H.W., N.M., W.L.; Investigation: H.W., N.M., W.L.; Resources: Z.W.; Data curation: H.W.; Writing - original draft: H.W.; Writing - review & editing: Z.W.; Supervision: Z.W.; Funding acquisition: Z.W.

Funding

This research received no specific grant from any funding agency in the public, commercial or not-for-profit sectors.

Data availability

The data sets used or analysed in this study are available from the corresponding author on reasonable request.

References

- Ambros, V. (2004). The functions of animal microRNAs. *Nature* **431**, 350-355. doi:10.1038/nature02871
- Bartels, C. L. and Tsonalis, G. J. (2009). MicroRNAs: novel biomarkers for human cancer. *Clin. Chem.* **55**, 623-631. doi:10.1373/clinchem.2008.112805
- Bogenrieder, T. and Herlyn, M. (2003). Axis of evil: molecular mechanisms of cancer metastasis. *Oncogene* **22**, 6524-6536. doi:10.1038/sj.onc.1206757
- Cai, J., Tian, A.-X., Wang, Q.-S., Kong, P.-Z., Du, X., Li, X.-Q. and Feng, Y.-M. (2015). FOXF2 suppresses the FOXC2-mediated epithelial-mesenchymal transition and multidrug resistance of basal-like breast cancer. *Cancer Lett.* **367**, 129-137. doi:10.1016/j.canlet.2015.07.001
- Chae, Y.-C., Kim, J.-Y., Park, J. W., Kim, K.-B., Oh, H., Lee, K.-H. and Seo, S.-B. (2019). FOXO1 degradation via G9a-mediated methylation promotes cell proliferation in colon cancer. *Nucleic Acids Res.* **47**, 1692-1705. doi:10.1093/nar/gky1230
- Chen, Y.-F., Wei, Y.-Y., Yang, C.-C., Liu, C.-J., Yeh, L.-Y., Chou, C.-H., Chang, K.-W. and Lin, S.-C. (2019). miR-125b suppresses oral oncogenicity by targeting the anti-oxidative gene PRXL2A. *Redox Biol.* **22**, 101140. doi:10.1016/j.redox.2019.101140
- Christiansen, J. J. and Rajasekaran, A. K. (2006). Reassessing epithelial to mesenchymal transition as a prerequisite for carcinoma invasion and metastasis. *Cancer Res.* **66**, 8319-8326. doi:10.1158/0008-5472.CAN-06-0410
- Feng, Y., Sun, T., Yu, Y., Gao, Y., Wang, X. and Chen, Z. (2018). MicroRNA-370 inhibits the proliferation, invasion and EMT of gastric cancer cells by directly targeting PAQR4. *J. Pharmacol. Sci.* **138**, 96-106. doi:10.1016/j.jphs.2018.08.004
- Gheldof, A. and Berx, G. (2013). Cadherins and epithelial-to-mesenchymal transition. *Prog. Mol. Biol. Transl. Sci.* **116**, 317-336. doi:10.1016/B978-0-12-394311-8.00014-5
- He, L., Thomson, J. M., Hemann, M. T., Hernando-Monge, E., Mu, D., Goodson, S., Powers, S., Cordon-Cardo, C., Lowe, S. W., Hannon, G. J. et al. (2005). A microRNA polycistron as a potential human oncogene. *Nature* **435**, 828-833. doi:10.1038/nature03552
- He, L., He, X., Lim, L. P., de Stanchina, E., Xuan, Z., Liang, Y., Xue, W., Zender, L., Magnus, J., Ridzon, D. et al. (2007). A microRNA component of the p53 tumour suppressor network. *Nature* **447**, 1130-1134. doi:10.1038/nature05939

- Herszényi, L., Hritz, I., Lakatos, G., Varga, M. Z. and Tulassay, Z. (2012). The behavior of matrix metalloproteinases and their inhibitors in colorectal cancer. *Int. J. Mol. Sci.* **13**, 13240-13263. doi:10.3390/ijms131013240
- Higashimori, A., Dong, Y., Zhang, Y., Kang, W., Nakatsu, G., Ng, S. S. M., Arakawa, T., Sung, J. J. Y., Chan, F. K. L. and Yu, J. (2018). Forkhead Box F2 suppresses gastric cancer through a novel FOXF2-IRF2BPL- β -catenin signaling axis. *Cancer Res.* **78**, 1643-1656. doi:10.1158/0008-5472.CAN-17-2403
- Hornebeck, W., Emonard, H., Monboisse, J.-C. and Bellon, G. (2002). Matrix-directed regulation of pericellular proteolysis and tumor progression. *Semin. Cancer Biol.* **12**, 231-241. doi:10.1016/S1044-579X(02)00026-3
- Iwai, N., Yasui, K., Tomie, A., Gen, Y., Terasaki, K., Kitaichi, T., Soda, T., Yamada, N., Dohi, O., Seko, Y. et al. (2018). Oncogenic miR-96-5p inhibits apoptosis by targeting the caspase-9 gene in hepatocellular carcinoma. *Int. J. Oncol.* **53**, 237-245. doi:10.3892/ijo.2018.4369
- Jiang, L., Lv, L., Liu, X., Jiang, X., Yin, Q., Hao, Y. and Xiao, L. (2019). MiR-223 promotes oral squamous cell carcinoma proliferation and migration by regulating FBXW7. *Cancer Biomark.* **24**, 325-334. doi:10.3233/CBM-181877
- Kao, Y.-Y., Chou, C.-H., Yeh, L.-Y., Chen, Y.-F., Chang, K.-W., Liu, C.-J., Fan Chiang, C.-Y. and Lin, S.-C. (2019). MicroRNA miR-31 targets SIRT3 to disrupt mitochondrial activity and increase oxidative stress in oral carcinoma. *Cancer Lett.* **456**, 40-48. doi:10.1016/j.canlet.2019.04.028
- Kaufmann, E. and Knöchel, W. (1996). Five years on the wings of fork head. *Mech. Dev.* **57**, 3-20. doi:10.1016/0925-4773(96)00539-4
- Klein, G., Vellenga, E., Fraaije, M. W., Kamps, W. A. and de Bont, E. S. J. M. (2004). The possible role of matrix metalloproteinase (MMP)-2 and MMP-9 in cancer, e.g. acute leukemia. *Crit. Rev. Oncol. Hematol.* **50**, 87-100. doi:10.1016/j.critrevonc.2003.09.001
- Kundu, S. T., Byers, L. A., Peng, D. H., Roybal, J. D., Diao, L., Wang, J., Tong, P., Creighton, C. J. and Gibbons, D. L. (2016). The miR-200 family and the miR-183~96~182 cluster target Foxf2 to inhibit invasion and metastasis in lung cancers. *Oncogene* **35**, 173-186. doi:10.1038/onc.2015.71
- Leemans, C. R., Braakhuis, B. J. M. and Brakenhoff, R. H. (2011). The molecular biology of head and neck cancer. *Nat. Rev. Cancer* **11**, 9-22. doi:10.1038/nrc2982
- Liu, B., Zhang, J. and Yang, D. (2019). miR-96-5p promotes the proliferation and migration of ovarian cancer cells by suppressing Caveolae1. *J. Ovarian Res.* **12**, 57. doi:10.1186/s13048-019-0533-1
- Mottok, A., Jurinovic, V., Farinha, P., Rosenwald, A., Leich, E., Ott, G., Horn, H., Klapper, W., Boesl, M., Hiddemann, W. et al. (2018). FOXP1 expression is a prognostic biomarker in follicular lymphoma treated with rituximab and chemotherapy. *Blood* **131**, 226-235. doi:10.1182/blood-2017-08-799080
- Qiu, Y., Ma, X., Yang, X., Wang, L. and Jiang, Z. (2017). Effect of sodium butyrate on cell proliferation and cell cycle in porcine intestinal epithelial (IPEC-J2) cells. *In Vitro Cell. Dev. Biol. Anim.* **53**, 304-311. doi:10.1007/s11626-016-0119-9
- Ress, A. L., Stiegelbauer, V., Winter, E., Schwarzenbacher, D., Kiesslich, T., Lax, S., Jahn, S., Deutsch, A., Bauernhofer, T., Ling, H. et al. (2015). MiR-96-5p influences cellular growth and is associated with poor survival in colorectal cancer patients. *Mol. Carcinog.* **54**, 1442-1450. doi:10.1002/mc.22218
- Saito, T., Nishikawa, H., Wada, H., Nagano, Y., Sugiyama, D., Atarashi, K., Maeda, Y., Hamaguchi, M., Ohkura, N., Sato, E. et al. (2016). Two FOXP3(+)/CD4(+) T cell subpopulations distinctly control the prognosis of colorectal cancers. *Nat. Med.* **22**, 679-684. doi:10.1038/nm.4086
- Shi, Z., Liu, J., Yu, X., Huang, J., Shen, S., Zhang, Y., Han, R., Ge, N. and Yang, Y. (2016). Loss of FOXF2 expression predicts poor prognosis in hepatocellular carcinoma patients. *Ann. Surg. Oncol.* **23**, 211-217. doi:10.1245/s10434-015-4515-2
- Simpson-Haidaris, P. J. and Rybarczyk, B. (2001). Tumors and fibrinogen. The role of fibrinogen as an extracellular matrix protein. *Ann. N. Y. Acad. Sci.* **936**, 406-425. doi:10.1111/j.1749-6632.2001.tb03525.x
- Sounni, N. E., Janssen, M., Foidart, J. M. and Noel, A. (2003). Membrane type-1 matrix metalloproteinase and TIMP-2 in tumor angiogenesis. *Matrix Biol.* **22**, 55-61. doi:10.1016/S0945-053X(03)00003-9
- Vahabi, M., Pulito, C., Sacconi, A., Donzelli, S., D'Andrea, M., Manciocco, V., Pellini, R., Paci, P., Sanguineti, G., Strigari, L. et al. (2019). miR-96-5p targets PTEN expression affecting radio-chemosensitivity of HNSCC cells. *J. Exp. Clin. Cancer Res.* **38**, 141. doi:10.1186/s13046-019-1119-x
- Vihinen, P. and Kähäri, V.-M. (2002). Matrix metalloproteinases in cancer: prognostic markers and therapeutic targets. *Int. J. Cancer* **99**, 157-166. doi:10.1002/ijc.10329
- Wang, B., Zhang, A., Zheng, J., Gong, J., Li, S., Zeng, Z. and Gan, W. (2011). Bufalin inhibits platelet-derived growth factor-BB-induced mesangial cell proliferation through mediating cell cycle progression. *Biol. Pharm. Bull.* **34**, 967-973. doi:10.1248/bpb.34.967
- Wang, Y.-G., Xu, L., Wang, T., Wei, J., Meng, W. Y., Wang, N. and Shi, M. (2015). Givinostat inhibition of hepatic stellate cell proliferation and protein acetylation. *World J. Gastroenterol.* **21**, 8326-8339. doi:10.3748/wjg.v21.i27.8326
- Wang, L., Chen, W., Zha, J., Yan, Y., Wei, Y., Chen, X., Zhu, X. and Ge, L. (2019). miR-543 acts as a novel oncogene in oral squamous cell carcinoma by targeting CYP3A5. *Oncol. Rep.* **42**, 973-990. doi:10.3892/or.2019.7230
- Warnakulasuriya, S. (2009). Global epidemiology of oral and oropharyngeal cancer. *Oral Oncol.* **45**, 309-316. doi:10.1016/j.oraloncology.2008.06.002

- Xu, W., San Lucas, A., Wang, Z. and Liu, Y.** (2014). Identifying microRNA targets in different gene regions. *BMC Bioinformatics* **15** Suppl. 7, S4. doi:10.1186/1471-2105-15-S7-S4
- Xu, Y. X., Sun, J., Xiao, W. L., Liu, Y. S., Yue, J., Xue, L. F., Deng, J., Zhi, K. Q. and Wang, Y. L.** (2019). MiR-4513 mediates the proliferation and apoptosis of oral squamous cell carcinoma cells via targeting CXCL17. *Eur. Rev. Med. Pharmacol. Sci.* **23**, 3821-3828.
- Yao, D., Dai, C. and Peng, S.** (2011). Mechanism of the mesenchymal-epithelial transition and its relationship with metastatic tumor formation. *Mol. Cancer Res.* **9**, 1608-1620. doi:10.1158/1541-7786.MCR-10-0568
- Zhang, Y., Wang, X., Wang, Z., Tang, H., Fan, H. and Guo, Q.** (2015). miR-182 promotes cell growth and invasion by targeting forkhead box F2 transcription factor in colorectal cancer. *Oncol. Rep.* **33**, 2592-2598. doi:10.3892/or.2015.3833